Catrina (2026), 37(1):1-15

Application of Ground Geophysical Methods for Delineating Mineralization Zones: A Case Study at Wadi Um Qeisum, Saint Catherine Area, Southern Sinai, Egypt

Remon N. Aziz[1*], Mohamed H. Yousef[1], Adel F. Khalel[1], Salah M. Hanafy[1], Motoyuki Sato[2,3], El-Arabi H. Shendy[4]

[1] Exploration Division, Nuclear Materials Authority, P.O. Box: 530, Maadi, Cairo, Egypt.
[2] Graduate School of Environmental Studies, Tohoku University, Sendai, Japan
[3] Center for Northeast Asian Studies, Tohoku University, Sendai, Japan.
[4] Geology Department, Faculty of Science, Suez Canal University, Ismailia 41522, Egypt

Received: October 26, 2025; Accepted: March 26, 2026; Published online: April 16, 2026

ABSTRACT

Wadi Um Qeisum, located in the Saint Catherine region of southern Sinai, Egypt, lies within the Arabian-Nubian Shield and hosts diverse natural mineral resources, including copper, rare earth elements (REEs), and radioactive minerals. This study integrates ground magnetic surveys, gamma-ray spectrometry, and self-potential (SP) techniques to outline mineralized zones and assess their structural influences. Magnetic data were analyzed using reduction to the pole (RTP), residual-regional separation, first vertical derivative (FVD), total derivative (TDR), horizontal gradient magnitude (HGM), Euler deconvolution (structural index, SI = 0), and source parameter imaging (SPI). These enhancements revealed faults, dykes, and contacts that govern mineralization, characterized by dominant NW-SE and NE-SW trends. Gamma-ray spectrometry revealed irregularities in the distributions of equivalent uranium (eU), equivalent thorium (eTh), and ^{40}K. Derived ratios (eU/eTh, eU/K, U-index, F-parameter) and ternary diagrams further highlighted zones of hydrothermal alteration and potential rare earth element (REE) enrichment. Radiometric anomalies correlate with the margins of intermediate dykes, altered quartz monzonite, and structural intersections. Self-potential (SP) data from 16 profiles defined three zones: pronounced negative anomalies (<−10.0 mV) associated with significant metallic mineralization; intermediate anomalies (-10.0 to -2.0 mV) linked to structural features; and positive anomalies (>-2.0 mV) indicative of unmineralized, resistive bedrock.

Quantitative modeling revealed shallow sources at 9-14 m depth, with low dips and limited lateral extent. Integration of these techniques precisely defines subsurface target sites, supporting targeted mineral exploration.

Key Words: Arabian-Nubian Shield; Ground magnetic; Gamma ray spectrometry; Radiometric anomalies; Rare earth elements (REE); Wadi Um Qeisum.

INTRODUCTION

Wadi Um Qeisum, located in the Saint Catherine region of the Sinai Peninsula, Egypt, forms part of the Arabian-Nubian Shield (ANS) and is recognized for its diverse mineralization hosted predominantly within Precambrian crystalline basement rocks (Shalaby *et al.*, 2005). The area is dominated by granitic and metamorphic lithologies that have undergone extensive tectonic distortion and hydrothermal alteration, resulting in the enrichment of various metallic minerals, including copper, lead, and zinc (Hilmy and Mohsen, 1965, 1966; Niazy *et al.*, 1995; El Aref *et al.*, 1999; Salem *et al.*, 2007).

The Saint Catherine region and its surroundings encompass multiple sites of secondary copper mineralization hosted within both basement rocks and overlying Phanerozoic sedimentary sequences. Prominent localities include Um Qeisum, El Regeita, Rahaba, Wadi Feiran, Sarabit El-Khadem, and Wadi Maghara (El-Ghawaby *et al.*, 1989).

Mineralization is structurally controlled and closely associated with shear zones and fault structures, which acted as conduits for metal-bearing hydrothermal fluids responsible for significant ore deposition (Helmy and Kaindl, 2002).

In addition to base metals, the region hosts gold-bearing veins and rare earth element (REE) mineralization, further enhancing its economic significance. REE mineralization is principally confined to granitic bodies and associated pegmatites widely distributed throughout southern Sinai (Abu El-Ela and Mohamed, 2015).

The study area lies within a well-documented mineralized zone that has attracted considerable scientific attention due to the presence of copper occurrences and its geological similarity to adjacent deposits (Hilmy and Mohsen, 1965, 1966; Niazy *et al.*, 1995; Salem *et al.*, 2007). Furthermore, correlations between radioactive anomalies and copper mineralization reported in neighbouring areas (Mousa *et al.*, 2014; Yousef, 2024) emphasize the metallogenic potential and structural continuity of the region.

Ground geophysical methods provide effectively tools for subsurface exploration and mineral targeting in such complex geological environments. Magnetic surveys are particularly valuable for delineating subsurface structures and identifying sulfide-rich zones

* *Corresponding author e-mail*: Remon.Aziz@science.suez.edu.eg.

associated with magnetic anomalies. Although rare earth elements are typically non-magnetic, they frequently occur in association with magnetic minerals such as magnetite or within lithological units that exhibit distinct magnetic signatures. Consequently, magnetic data can indirectly indicate favorable zones for REE mineralization, particularly in geological settings such as peralkaline granites and carbonatites (Li *et al.*, 2018).

Gamma-ray spectrometry, whether airborne or ground-based, measures the concentrations of naturally occurring radioactive elements, such as potassium (K), equivalent uranium (eU), and equivalent thorium (eTh) in rocks and soils. The spatial distribution and ratios of these elements (K/eTh and eU/eTh) provide critical understandings of lithological variations and hydrothermal alteration zones, which are often spatially associated with mineralization. Although this method does not directly detect base metals, it effectively delineates alteration halos and geological environments favorable for copper, lead, and zinc deposits (Gobashy *et al.*, 2024; Azzazy, 2023). Moreover, REE-bearing minerals are commonly associated with thorium- and uranium-rich phases, creating gamma-ray spectrometry a valuable indirect exploration tool for REE deposits (El Ghrabawy *et al.*, 2021; Abd El-Rahman *et al.*, 2024; González *et al.*, 2018). Moreover, REE-bearing minerals are commonly associated with thorium- and uranium-rich phases, making gamma-ray spectrometry a valuable indirect exploration tool for REE deposits (El Ghrabawy *et al.*, 2021; Abd El-Rahman *et al.*, 2024; González *et al.*, 2018).

The self-potential (SP) method, which measures naturally occurring electrical potentials at the Earth's surface, is widely applied in detecting subsurface mineralization, particularly sulfide deposits. Variations in electrical potential are often linked to electrochemical processes associated with ore bodies and can provide indirect indications of mineralization and element deposites (Santos *et al.*, 2016). The integration of magnetic, gamma-ray spectrometric, and self-potential methods enables a comprehensive characterization of subsurface geological conditions, facilitating the delineation of mineralized zones and improving exploration efficiency (Ribeiro *et al.*, 2020). Accordingly, the objectives of the present study are: 1, to conduct ground magnetic surveys to delineate geological structures controlling mineralization, including faults and intrusive bodies, and to identify magnetic anomalies indicative of potential ore deposits; 2, to utilize ground gamma-ray spectrometry to map the spatial distribution of potassium, uranium, and thorium and to identify anomalous zones associated with hydrothermal alteration and mineralization; and 3, to apply the self-potential (SP) method to investigate anomalous subsurface extensions of surface mineralization and to define their lateral and vertical continuity.

Through the integration of these geophysical techniques, this study aims to provide a comprehensive understanding of the structural and lithological controls on mineralization within the study area.

MATERIALS AND METHODS

Study Area and its Geological Characterization

Wadi Um Qeisum (Fig.1A), located in the Saint Catherine region of southern Sinai, Egypt, with coordinates of approximately 28°32′N, 33°55′E. It is geologically situated within the northwestern margin of the Arabian-Nubian Shield (ANS). The ANS characterises by an extensive Neoproterozoic terrane spanning northeastern Africa and the western Arabian Peninsula (Stern, 1994). This shield primarily comprises ancient igneous and metamorphic rocks formed through the accretion of volcanic arcs and microcontinents during the late Neoproterozoic (~900-550 Ma) (Johnson *et al.*, 2011).

The Um Qeisum region is predominantly composed of quartz monzonite rock (Fig. 1B). It encompasses a vast area of rocky Mountains intersected by the NE-SW-trending fault that delineates Wadi Um Qeisum. The rock exhibits have an inequigranular porphyritic texture in thin sections, characterized by phenocrysts of plagioclase and quartz embedded in an inequigranular groundmass (Azer, 2007; Salem and El-Fouly, 2000). The northwestern region of the research area is comprised of fresh alkali feldspar granites, whereas the southeastern region has quartz monzonite rocks. The studied region is intersected by basic and intermediate dykes predominantly oriented in the WNW-ESE and NNE-SSW axes (Arnous, 2000; Abuzied, 2011).

Several structural lineaments traverse the area in multiple directions; however, two predominant sets of faults constitute the main structural framework. The first set comprises a series of elongated parallel fault planes oriented in the NE-SW and NNE-SSW directions, aligned with the Gulf of Aqaba. The second set is oriented parallel to the Gulf of Suez in a west-northwest to east-southeast orientation. A less frequent set of faults extends in the North-South direction (Rashed and Shendi, 2022).

Ground Magnetic Survey

The ground magnetic method is a prevalent geophysical technique employed to identify fluctuations in the Earth's magnetic field caused by surface and subsurface geological bodies having different mineral compositions. It is especially proficient at detecting lithological connections and structural features, including faults, shear zones, and folds, which are crucial for mineral exploration and geological mapping. The method depends on the contrasts in magnetic susceptibility across various rock types and has been substantially improved by advancements in magnetometer technology and data processing methodologies. Recent studies highlight its significance in identifying mineralized zones and subsurface structures, especially through the use of analytical methods such as the total horizontal derivative and the

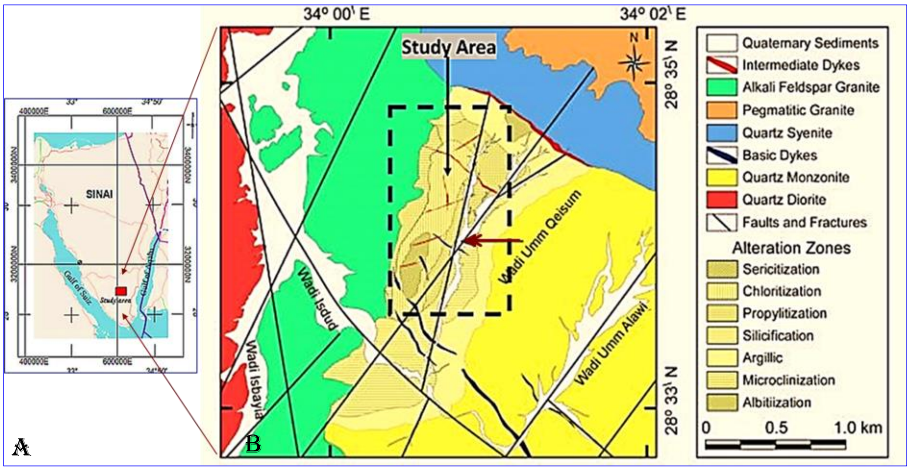

Figure (1): Location and geology of the study area. A, Regional map showing the position of the study area within the Sinai Peninsula, Egypt. B, Geological map of Wadi Um Qeisum illustrating the distribution of rock units, structural elements (faults and fractures), and associated alteration zones (Rashed and Shendi, 2022).

analytic signal (El Qot *et al.*, 2023). The integration of ground magnetic data with other geophysical datasets has demonstrated efficacy in identifying mineralized zones, particularly in structurally regulated ore systems (Benhamou *et al.*, 2024). These advancements underscore the method's sustained significance in geophysical investigations related to mineral and structural mapping.

The proton precession magnetometer is the most often utilized instrument for ground magnetic surveys. The magnetometer employed in the current survey is a proton magnetometer (model PMG1, Geofyzika, Brno, Czech Republic). A systematic ground magnetic survey was conducted in the research area along north-south profiles, utilizing a grid design with 40m line spacing and 20m station separation.

Ground Gamma-Ray Spectrometry Survey

Gamma-ray spectrometry is an essential geophysical technique used to measure the natural gamma radiation emitted by isotopes of potassium (K^{40}), uranium (eU), and thorium (eTh) in rocks and soils. This method provides valuable information for geological mapping, mineral exploration, and evaluating ambient radioactivity. By analyzing the energy and intensity of gamma rays, it enables the identification and spatial distribution of radiogenic materials, which indicate lithological changes and structural characteristics. In geophysics, gamma-ray spectrometry is highly advantageous due to its non-destructive characteristics, elevated sensitivity, and capacity to efficiently survey large areas, particularly when utilized in airborne surveys. Recent studies have underscored its significance in defining geotectonic environments, charting alteration zones, and assessing radiological risks across diverse geological contexts (Al Rawahi *et al.*, 2022; Ouadif *et al.*, 2022; Abd El-Rahman *et al.*, 2024). These applications illustrate the method's essential function in contemporary geophysical studies and resource evaluations.

In the current study region, systematic ground gamma-ray spectrometric measurements were conducted along the identical grid patterns of the ground magnetic survey. Gamma-ray measurements were conducted with a portable hand-held radiation spectrometer, model GS-512i. The survey data includes the total count T.C (Ur), equivalent uranium (eU in ppm), equivalent thorium (eTh in ppm), and potassium (K in %). The data were adjusted for background and stripping ratios to derive the net concentrations of the three radioelements and the total gamma ray count.

The processed measurements were presented as color radioactivity maps for TC, eU, eTh, K, eU/eTh, eU/K, uranium-index, and F-parameter, along with a false-color composite image of eU, eTh, and K% utilizing the Geosoft program (Geosoft, 2014).

Self-Potential (SP) Survey

The self-potential (SP) method is a passive geophysical technique that measures natural voltage differentials at the Earth's surface, primarily generated by electrochemical and electrokinetic processes occurring in the subsurface. In mineral exploration, it is particularly effective for identifying conductive ore deposits like sulfides, which generate distinctive SP anomalies resulting from redox reactions and fluid flow interactions. Electrochemical sources are commonly related the oxidation of metallic minerals, whereas electrokinetic sources originate from the flow of groundwater through permeable rock formations. The SP approach has garnered fresh attention owing to its cost-effectiveness, non-invasive characteristics, and capacity to enhance other geophysical techniques. Recent studies have shown its effectiveness in identifying mineralized zones and mapping subsurface structures, especially when combined with magnetic and resistivity surveys (Abdelsalam *et al.*; 2024, Yousef, 2024). The method's sensitivity to hydrothermal and electrochemical activity renders it an indispensable instrument in contemporary mineral exploration initiatives.

This methodology illustrates polarization phenomena occurring at depth. Significant negative self-potential anomalies associated with mineral deposits have been identified since the nineteenth century. For example, Fox (1830), Church (1984), Elkattan *et al.* (1996), Bigalke *et al.* (2004), Sultan *et al.* (2009), Mousa *et al.* **(**2014), Assran *et al.* (2018), Horo *et al.* (2023), Abdelsalam *et al.* (2024), and Yousef (2024).

RESULTS

Ground magnetic data

Reduction to the pole (RTP), residual, and regional component maps

The terrestrial magnetic data were adjusted for diurnal fluctuations, normal-field adjustment to account for expected changes in geomagnetic field intensity based on latitude and longitude (Sharma, 1997), and tie-line correction.

Due to the inclination of the Earth's magnetic field, magnetic anomalies frequently exhibit both positive and negative responses, with their peaks displaced from the source along the magnetic meridian. At an inclination of 90°, the anomaly is positioned directly above the source. The Reduction to the Pole (RTP) technique is employed to rectify this offset, adjusting the data as though it were recorded at the magnetic pole, so aligning the magnetic highs with their sources (Kearey and Brooks, 1991). The total intensity magnetic map (Fig. 2a) was reduced to the pole (Fig. 2b) utilizing the area's known inclination (42.8°) and declination (4.6°).

Magnetic data provide the aggregate magnetic fields from all subterranean sources. Analyzing these data enhances subsurface imaging and geological interpretation. The application of several processing approaches typically results in more dependable conclusions, supported by diverse numerical interpretation methods (Pour *et al.*, 2023).

Magnetic data obtained from geological surveys reflect the aggregate magnetic fields from all subsurface sources. Many surveys, however, concentrate on small-scale, superficial structures, whose magnetic signals are frequently obscured by a more extensive regional field originating from larger or deeper sources. To isolate the target signals, the regional field must be assessed and eliminated from the overall magnetic data. This study employed a Fast Fourier Transform (FFT) on the RTP magnetic data using Geosoft (2014) to examine frequency content and establish a suitable cut-off frequency for producing high-pass and low-pass filtered maps (Fig. 2C).

The visual examination of the 2D power spectrum (Fig. 2C) identified two different linear segments, which were fitted to individual shallow and deep source components. This study produced high-pass (residual) and low-pass (regional) magnetic maps (Figs. 3A and 3B) by band-pass filtering (Geosoft, 2014). The estimated average depths for the shallow and deep magnetic sources, derived from the power spectrum curve, are around 20 meters and 60 meters, respectively.

The RTP magnetic data underwent additional processing through various techniques, including first-order vertical derivative (FVD) and tilt derivative (TDR), to enhance and delineate near-surface lineament structures such as faults, contacts, dykes, and shear zones, which are often pivotal in the localization of mineral deposits.

First vertical derivative (FVD) and tilt derivative (TDR)

Lineaments are surface manifestations of subsurface discontinuities, including faults, fractures, and joints. Accurate mapping of these features often reveals the fundamental structural framework of a region. Thus, lineament analysis is a crucial instrument for elucidating historical tectonic processes and is significant in the exploration of mineral resources, petroleum, and groundwater (Mostafa and Zakir, 1996).

The First Vertical Derivative (FVD) approach is particularly effective for emphasizing shallow magnetic characteristics due to its heightened sensitivity to near-surface sources. (Fig. 4A) It enhances high-frequency elements in the data, hence enhancing the resolution of minor geological formations. Zero-contour lines on the FVD map facilitate the distinction between different lithological and structural units (Fig. 4A). The first vertical derivative of T(x, y, z) with regard to z can be articulated as:

$$(T(x, y, z)): \frac{\partial f}{(\partial z)}$$

Where, ƌ displays the FVD map obtained from the magnetic data.

The Tilt Derivative (TDR) technique is widely used to delineate shallow basement structures and has proven effective in mineral exploration.

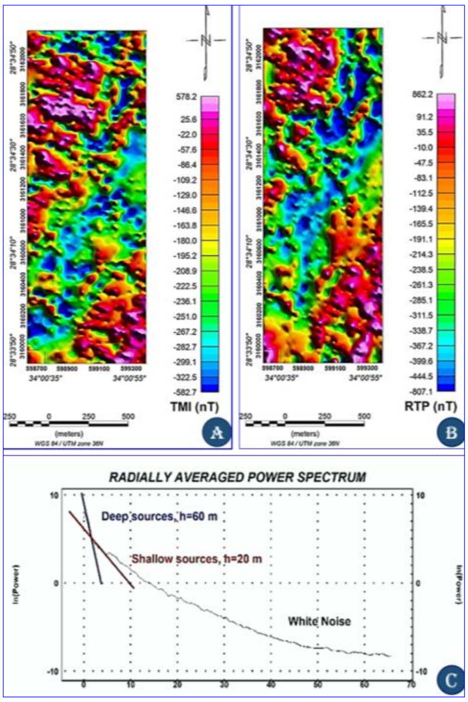

Figure (2): Total magnetic intensity (TMI) and reduced-to-pole (RTP) maps, along with the radially averaged power spectrum of RTP data, revealing subsurface structural features and source depths in Wadi Um Qeisum, Southern Sinai, Egypt: (A) TMI map, (B) RTP map, and (C) power spectrum curve.

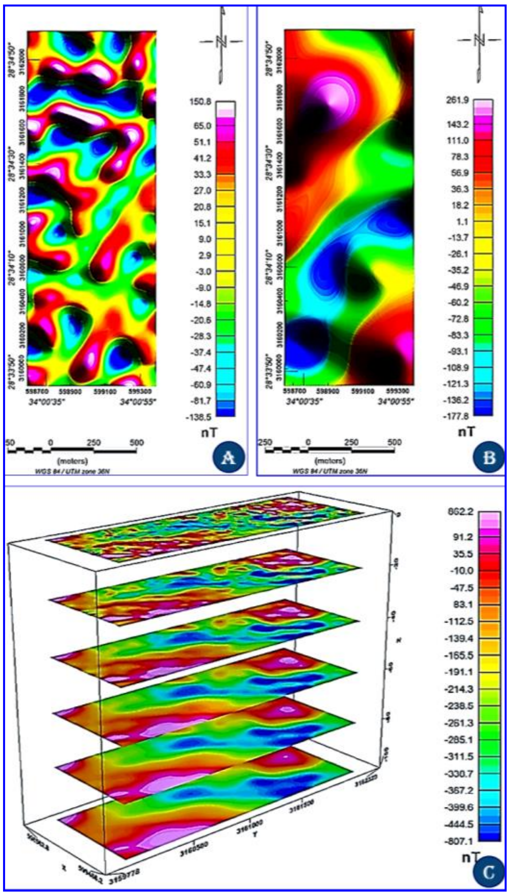

Figure (3): Magnetic field separation and upward continuation of RTP data for subsurface interpretation, Wadi Um Qeisum, Southern Sinai, Egypt. A, Residual magnetic anomaly map emphasizing shallow sources and short-wavelength features. B, Regional magnetic field map reflecting deep-seated sources and long-wavelength anomalies. C, Upward continued RTP maps (20-100 m) showing attenuation of shallow effects and enhancement of deeper magnetic structures.

However, it is less effective in resolving deep-seated sources, as their boundaries often fail to generate well-defined TDR responses. Miller and Singh (1994) defined the calculated TDR as follow:

$$\text{TDR} = \arctan\left(\frac{VDR}{HGM}\right)$$

Where, VDR denotes the vertical derivative of the magnetic field, while HGM represents its horizontal gradient magnitude.

By applying a zero threshold to the TDR field and delineating the corresponding zero-contour, the boundaries between positive and negative tilt values can be clearly defined, thereby facilitating the identification of zones associated with positive magnetic anomalies and enhancing the delineation of shallow structural features.

Horizontal Gradient Magnitude (HGM)

The horizontal gradient magnitude (HGM) of ground magnetic data is a widely used technique in magnetic data processing, especially for identifying the boundaries of shallow magnetic sources such as faults, dykes, or contacts. It highlights lateral variations in the magnetic field by emphasizing areas of high gradient, facilitating the interpretation of subsurface structures (Fig. 4C). Blakely (1995) states that if T(x,y) denotes the observed magnetic field at the surface, then the following equation should be followed:

$$HGM = \sqrt{\left[\left(\frac{\delta T}{\delta x}\right)^2 + \left(\frac{\delta T}{\delta y}\right)^2\right]}$$

Where, HGM is horizontal gradient of magnetic map for the research area; T, is magnetic field intensity; $\partial T/\partial x$, is rate of change of magnetic intensity in the X-direction; $\partial T/\partial y$, is rate of change of magnetic intensity in the Y-direction.

The rose diagrams generated from ground magnetic data (Figs. 5A-E) illustrate the orientation and frequency of magnetic lineaments, highlighting predominant structural features such as faults and fractures that affect the area's magnetic signature (Geriesh, et. al.,2025). These trends are significant as they frequently govern the deposition and concentration of mineralization.

Euler deconvolution and source parameter imaging (SPI)

Euler Deconvolution, formulated by Reid *et al.* (1990), employs gridded magnetic data to ascertain the locations and depths of magnetic sources. This technique has been extensively utilized for the identification of geological formations, including faults and contacts. The Euler Deconvolution equation is articulated as follows:

$$N(B - T) = \partial T/\partial x\,(x - x_0) + \partial T/\partial y\,(y - y_0) + \partial T/\partial z\,(z - z_0)$$

Where, N indicates the structural index (SI) and which illustrates the geometry of the source.; B signifies the regional background magnetic field, T represents the observed total magnetic field at the coordinates (x, y, z), (x_0, y_0, z_0) denotes the position of the magnetic source.

In this study, Euler solutions were generated using a structural index (SI) of 0, which is typically employed to delineate geological contacts. with the results illustrated in figures (6A). Enhancements to this approach that aimed at improving its applicability to magnetic datasets, were proposed by Barbosa *et al.* (1999).

Source Parameter Imaging (SPI) is a depth estimate method that applies the principle of the complex analytic signal to magnetic data, utilizing the local wavenumber. It is relevant to two-dimensional models, including dipping contacts and thin sheets. Thurston and Smith (1997) define the local wavenumber K as follows:

$$K = \frac{[(\partial^2 M/\partial x\partial z)(\partial M/\partial x) - (\partial^2 M/\partial x^2)(\partial M/\partial z)]}{[(\partial M/\partial x)^2 + (\partial M/\partial z)^2]}$$

Where, M is the magnetic field intensity in the study area. x, zm are spatial coordinates, usually horizontal (x) and vertical/depth (z); $\partial M/\partial x$, is first derivative of M along the x-direction, rate of change of M horizontally; $\partial M/\partial z$, is first derivative of M along the z-direction, rate of change of M with depth; $\partial^2 M/\partial x^2$, is second derivative along x, how the horizontal slope changes along x, $\partial 2M/\partial x\partial z$, is Mixed second derivative, how the horizontal slope changes with depth.

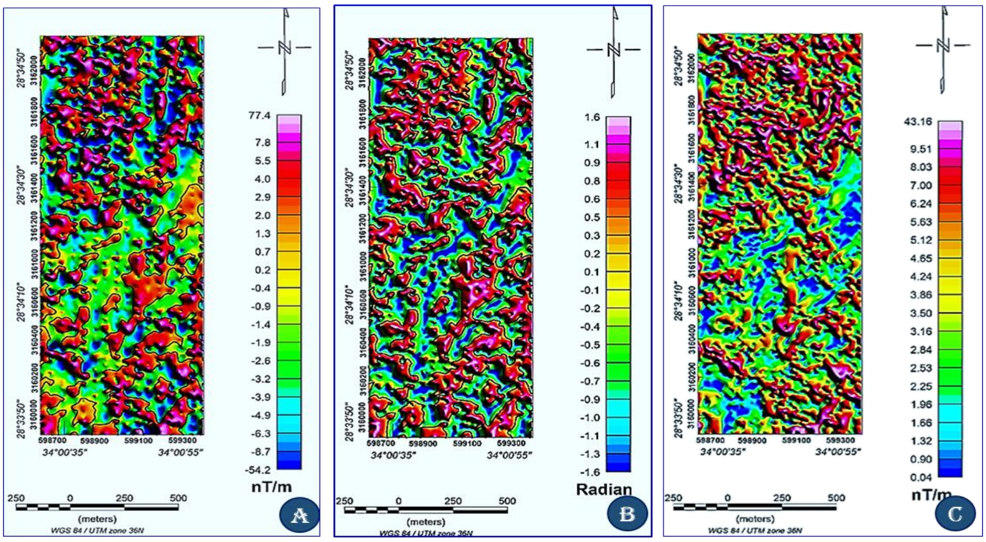

Figure (4): Magnetic derivative maps of the study area, Wadi Um Qeisum, Southern Sinai, Egypt. A, First vertical derivative (FVD) map highlighting shallow magnetic sources; B, Tilt Derivative (TDR) map showing anomaly edges and C, horizontal gradient magnitude (HGM) map allocating structural boundaries and contacts.

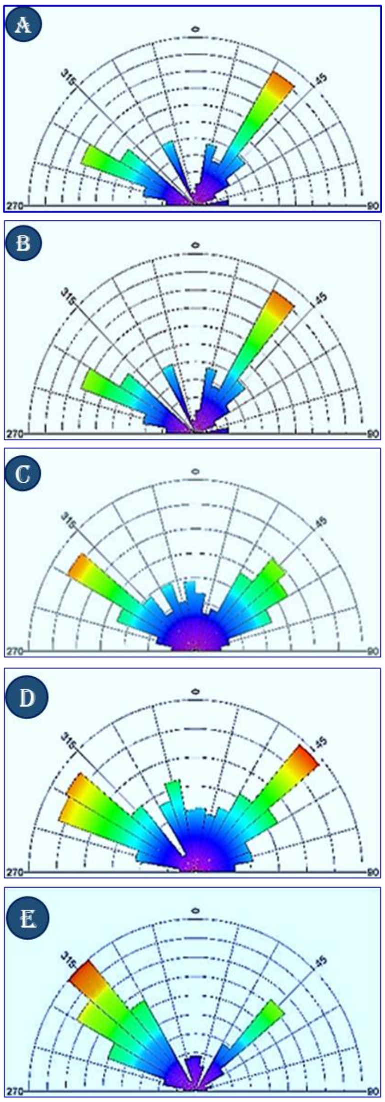

Figure (5): Rose diagrams of structural lineaments from geophysical map derivative maps in Wadi Um Qeisum, Southern Sinai, Egypt. A, Residual magnetic component map; B, regional magnetic component map; C, first vertical derivative (FVD) map; D, tilt derivative (TDR) map; and (E) horizontal gradient (HG) map.

The maximum of K for dipping contacts occur directly above the contact edges and are unaltered by magnetic inclination, declination, dip, strike, or remanent magnetization. The depth to the magnetic source can be approximated by the inverse of the peak wave number.

$$\text{Depth } (x = 0) = 1 / K_{max}$$

Where, K_{max} denotes the maximum value of the local wavenumber throughout the source. Figure (6B) displays the depth estimations derived from the SPI approach.

Gamma-Ray Spectrometric Data

The four radiometric maps (Figs. 7A-D) exhibit varying levels over the investigated area, indicating a disparity in radioelement concentrations among the different rock types present. This variety indicates a diverse distribution of radioactive materials, potentially linked to structural characteristics like faults or alteration zones. The TC, eU, eTh, and K% maps (Figs. 7A-D) of the investigated area exhibit a broad spectrum of radioactivity, with values ranging from roughly 11.6 to 120.4 Ur, 0.2 to 58.4 ppm, 2.0 to 103.0 ppm, and 1.2 to 7.9%, respectively.

The ratios eU/eTh and eU/K are extensively employed in gamma-ray spectrometric surveys for uranium deposit exploration, as they assist in identifying zones exhibiting anomalous uranium concentrations (Fig. 8A-D). The eU/eTh ratio is particularly significant due to thorium (Th) being largely stationary under most geological circum-stances, but uranium (U) is more mobile and can be transferred and reprecipitated by hydrothermal solutions or groundwater. An increased eU/eTh ratio typically signifies uranium enrichment or remobilization, serving as an effective factor for differentiating between primary and secondary uranium sources (Darnley, 1973; Boyle, 1982). Conversely, the eU/K ratio evaluates the uranium level relative to potassium (K), a prevalent element found in various rock-forming minerals like feldspar and mica. An elevated eU/K ratio may indicate hydrothermal alteration or weathering processes that have incorporated uranium into the rock matrix, especially in felsic or metamorphic environments. These ratios are particularly efficacious when combined with geological, geochemical, and structural data to identify probable areas for uranium mineralization (Grasty *et al.*, 1985).

The eU/eTh and eU/K ratios for the research area were illustrated using color ratio maps (Figs. 8A-B). In natural geochemical equilibrium, the usual background values for the eU/eTh ratio range from about 0.2 to 0.6, indicating the relative immobility of thorium compared to uranium. Anomalous levels are typically seen as commencing around 0.7, with numbers surpassing 1.0-1.2 signifying notable uranium enrichment, frequently resulting from mobilization and redeposition in oxidizing environ-ments (Darnley, 1973; Boyle, 1982; Grasty and Cox, 1997). Figure (8A) depicts the eU/eTh ratio map, with contour lines delineating areas exceeding 0.5. The eU/K ratio, indicating the relative quantity of U to K, often exhibits background values between 0.5 and 1.0. abnormal zones are identified when the ratio surpasses 1.5, with values exceeding 2.0 deemed very abnormal, frequently indicating K depletion (due to sericite-ization) or uranium enrichment via hydrothermal solutions (IAEA, 2003; Wilford, 2012). The contour lines in the eU/K ratio map delineate locations exceeding 2.0 (Fig. 8B).

Saunders and Potts (1978), attempted to determine a general uranium favorability index by plotting the histograms of various possible indices, such as the eU/eTh ratio for about 30 different areas, where the existing mines and occurrences were known to be favorable. It is articulated as:

U-index = (eTh *K) / eU

The U-Index (Fig.8C) emphasizes regions of U enrichment in comparison to the geochemically stable elements thorium and potassium. Increased values often signify secondary U-mobilization via hydrothermal processes, weathering, or redox reactions, whereas diminished values imply equilibrium or depletion (IAEA, 2003; Wilford, 2012; Drew *et al.*, 2013). It is particularly effective in detecting alteration zones and prospective mineralization in sedimentary, volcanic, and granitic environments. Typically, background values around 1, although levels over 1.5-2 are deemed unusual, andthose surpassing 3-4 may signify significant uranium mobilization (Grasty and Cox, 1997; IAEA, 2003; Wilford, 2012).

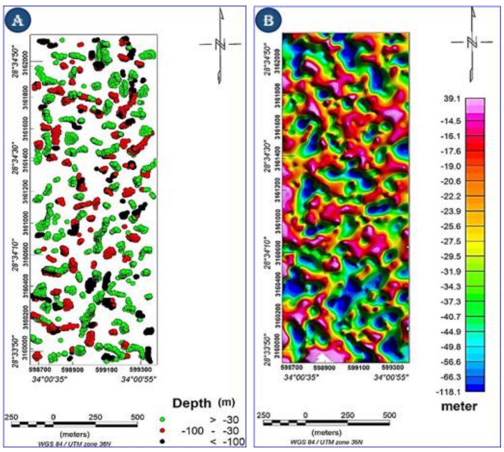

Figure (6): Depth estimation of magnetic sources in Wadi Um Qeisum, Southern Sinai, Egypt. (a) Euler deconvolution solutions using a structural index (SI = 0), display the spatial distribution of calculated source depths; (b) filled-color source parameter imaging (SPI) map showing the lateral variation in depth to magnetic sources across the study area.

Efimov (1978) created the F-parameter, a composite radiometric indicator derived from the relative abundances of potassium (K), uranium (U), and thorium (Th), to characterize the geochemical behavior of radioactive elements in geological formations. It is a metric intended to evaluate the comparative enrichment of uranium (eU) relative to thorium (eTh) and potassium (K) in geological formations. This approach assumes that different lithologies (Fig. 8D) and alteration types possess characteristic ratios of K-, U-, and Th-bearing minerals, resulting in unique gamma-ray spectrometric responses (Grasty and Cox, 1997; Wilford, 2012). Thus, abnormal F-values serve as significant indications of prospective ore zones, particularly when combined with geological, structural, and geochemical data in exploration initiatives (IAEA, 2010; Drew *et al.*, 2013). Efimov articulated the F-parameter through the subsequent equation:

F = K (eU /eTh)

Where, eU denotes equivalent uranium concentration (ppm); eTh signifies equivalent thorium concentration (ppm) and K represents potassium content (%).

Ternary radioelement maps maps represent essential tools for the rapid interpretation of gamma-ray spectrometric data, particularly when combined with geological and geophysical datasets (Minty *et al.*, 2009; IAEA, 2010). These maps illustrate the relative abundances of, uranium (U), thorium (Th) and potassium (K) through the use of red, green and blue, and color channels, respectively, providing a visual depiction of radioelement distribution (IAEA, 2003; Wilford, 2012). Reddish portions denote uranium -rich zones, bluish and greenish hues represent thorium- and potassium-enriched areas, white indicates balanced high concentrations, and dark parts signify low radioelement content (Fig. 9A). The uranium, thorium, and potassium maps were constructed to show the distribution of these elements relative to their ratios (Figs. 9A-D).

A map was generated to integrate the gamma-ray spectrometric data, delineating the greatest values as a contour line for eU/eTh, eU/K, uranium index, and F-parameter, as previously described (Fig. 10A). A map was created from the aggregate of these contours, illustrating the zones with the highest potential for mineral development, particularly for rare earth elements (REE) (Fig. 10B).

Self-Potential (SP) Data

The Self-Potential (SP) survey conducted in this study comprised along 16 north-south profiles, each measuring 200 meters in length, with a profile spacing

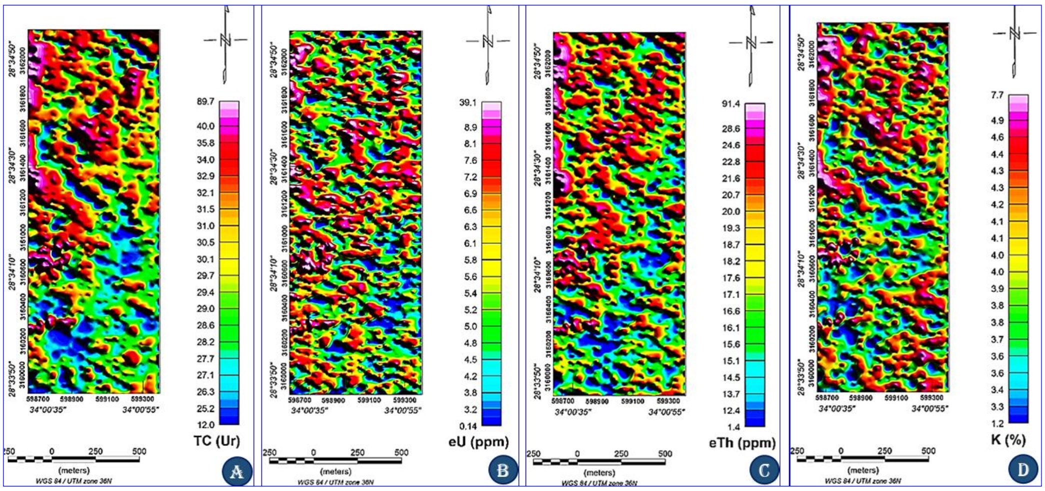

Figure (7): Gamma-ray spectrometric maps illustrating the spatial distribution of radiometric concentrations across different rock units in Wadi Um Qeisum, Southern Sinai, Egypt. A, Total count (TC) map expressed in uranium equivalent units (Ur); B, equivalent uranium (eU) map (ppm); (C) equivalent thorium (eTh) map (ppm); and (D) potassium (K) map (%).

and station interval of 20 meters. Furthermore, one chosen profile (tie line) was stretched by 300 meters. A particular station, situated at a highly steady SP potential point, was selected as the base station. All SP measurements were calibrated to this reference location. The equipment at the base station was calibrated to zero by connecting it to non-polarizing electrodes situated at the same location. All base station measurements were calibrated to correspond with the zero reference of a specified general base station encompassing the whole surveyed region. Concurrently, the second electrode (rolling electrode) traversed the grid stations to get field measurements, executed with an Auto-Ranging Digital Multimeter, Model HP 972A (manufactured in the USA).

The SP data were corrected by subtracting the base station value of each profile from the readings obtained at the corresponding stations. Electrode potential differences were deducted from the corresponding station values. The rectified SP data were subsequently utilized to produce a contour map for qualitative analysis. The adjusted SP values corresponding to specific anomalies were graphed against distance on millimeter paper to generate reduced SP anomaly profiles. These profiles were utilized to ascertain anomalous parameters with enhanced precision.

The SP contour map of the research area (Fig. 11) delineates abnormal zones potentially associated with mineralized regions influenced by structural characteristics. Generally, pronounced negative SP anomalies signify elevated concentrations of metallic mineralization, whereas positive SP responses are commonly linked to resilient, unmineralized areas.

In this work, six SP anomalies were chosen for quantitative analysis. The characteristics of the source anomaly were assessed utilizing the methodology of Ram Babu and Atchuta Rao (1988), which allows for the rapid and precise interpretation of the field profile. The adoption of this approach indicates that the depths of the inferred bodies responsible for the anomalies are superficial. These shallow sources, typically within 9-14 m, align well with the compact dimensions (9-15 m) and moderate polarization angles (10°-17°) observed across the profiles in Wadi Um Qeisum.

Quantitative interpretation of self-potential (SP) an-

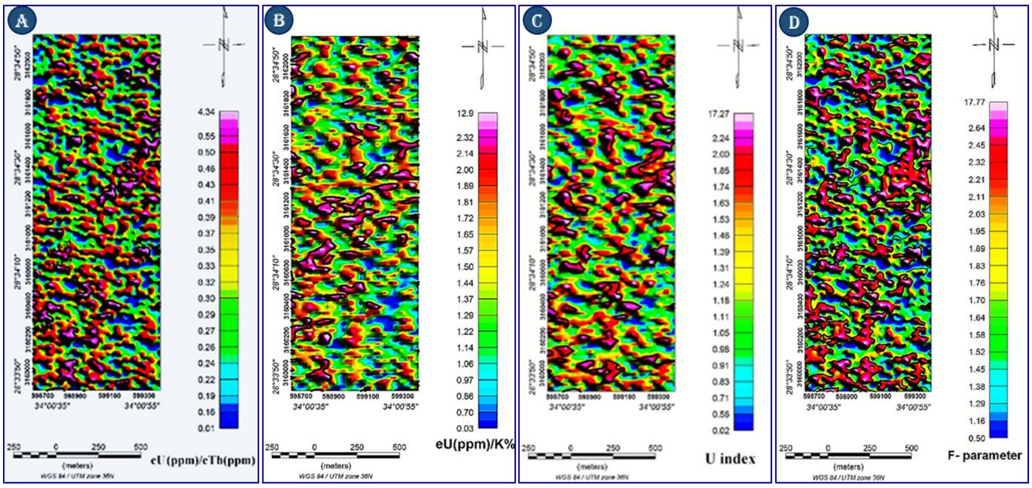

Figure (8): Derived Radiometric Ratio Maps (eU/eTh, eU/K%) and Uranium Enrichment Indicators (U-index and F-parameter) from Gamma-Ray Spectrometry, Wadi Um Qeisum, Southern Sinai, Egypt. A, eU/eTh map; B, eU/K% map; C, uranium index map, and D, F-parameter map, Wadi Um Qeisum, Southern Sinai, Egypt.

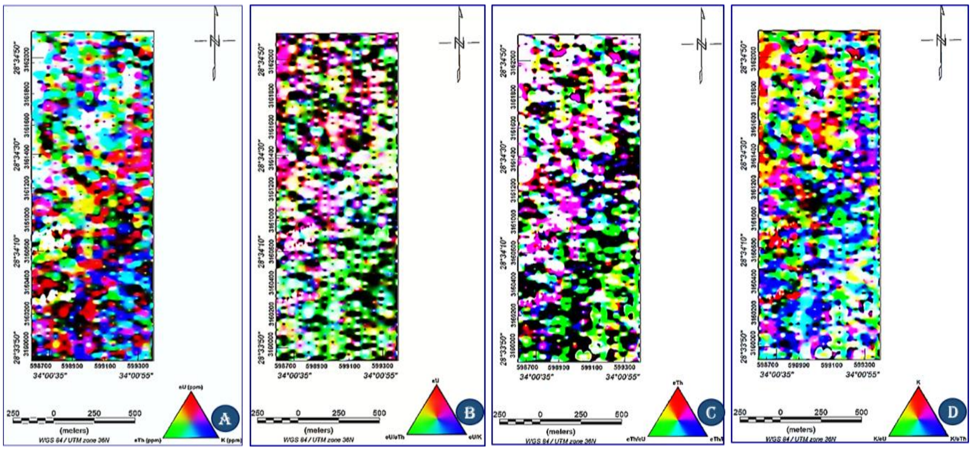

Figure (9): False-color composite images of Wadi Um Qeisum, Southern Sinai, Egypt. A, the three radioelement; B, uranium; C, thorium, and D, potassium.

omalies provides key insights into subsurface structures in Wadi Um Qeisum, Southern Sinai, Egypt. Table (1) summarizes results for six selected profiles, where polarization angles (θ) ranged from 10° to 17°, source depths (h) from 9 to 14 m below the surface, and body dimensions, half-width in meters, ranged from 9 to 15 m, indicating shallow, compact sources consistent with mineralization districts or fluid interfaces. Four anomalies are recognized: Profiles (1, 3, 5), is the first which dipped westward in alignment with regional structures, whereas others showed southward (Profile 2), northward (Profile 4), and eastward (Profile 6) dips, reflecting subsurface heterogeneity that may control ore deposition or groundwater pathways.

Table (1): Summary of quantitative interpretation of selected self-potential (SP) anomalies with consequential structural parameters (Dip Angle θ, Dip direction, Depth H, and Width A), Wadi Um Qeisum, Southern Sinai, Egypt.

profile No.	Calculated Parameters			
	θ (°)	Dipping direction	H (m)	A (m)
1	10	West	9	11
2	12	South	9	9
3	17	West	12	12
4	14	North	13	14
5	15	West	14	15
6	12	East	14	15

θ = Polarization angle in degrees.

DISCUSSION

Ground magnetic data

The visual examination of the RTP map indicates a predominant NW-elongation trend in the northwestern section of the research area, whereas a NE-elongation trend characterizes the remainder portion. The RTP map can be categorized into two zones based on the nature of magnetic anomalies. The first zone encompasses the northern and southeastern regions of the research area. It is characterized by high-amplitude positive magnetic anomalies with relatively high frequencies. This area may indicate rocks with elevated magnetic concentration at either shallow or profound depths. The second zone covering the central region of the research area, marked by a negative magnetic amplitude that intensifies toward the northeast. This area may indicate silicic rocks with poor magnetic properties associated with either shallow or deep origins. This may indicate a subduction zone originating from the northeast-southwest rift system linked to the Gulf of Aqaba's formation, which produced Wadi of Um Qeisum, recently obscured by Quaternary sediments.

The residual component map exhibits no distinct spatial correlation with the RTP map regarding the distribution of the identified zones, hence strengthening their link with deep rather than shallow sources. The residual map corresponds with the structural trends depicted in the RTP map, exhibiting NW and WNW tendencies in the NW section of the research region, and NE trends in the SE section. The anomalies on the residual map are predominantly elongated, accompanied by smaller oval-shaped positive and negative anomalies of diverse sizes and amplitudes. The regional component map exhibits a robust spatial correlation with the magnetic zones on the RTP map, confirming their association with deep-seated structures. The most elevated positive values are located in the NW and SE regions of the research area, suggesting potential sources of highly magnetic source rocks, whereas the center zone indicates the presence of deep, extremely acidic rocks. The visual examination of anomaly orientations on this map indicates prevailing NE and NW structural trends. To verify the separation method, upward continuation was implemented on the RTP data to produce depth slices at 20-meter intervals up to 100 meters. The initial slice represents the RTP map, and the findings indicate a remarkable resemblance between the deeper slices and the regional component map, so validating the separation's accuracy.

The FVD and TDR maps significantly enhance the understanding of near-surface magnetic features, providing valuable insights into the structural and lithological framework of the study area, an essential factor for mineral exploration and development. The FVD map identifies the boundaries of magnetic sources, facilitating the delineation of features such as faults, dykes, or lithological contacts that may serve as traps for mineralizing fluids. The TDR map integrates gradients from all directions to generate a continuous image that highlights both vertical and horizontal boundaries, facilitating the identification of intricate structures that may influence mineral deposition. A significant characteristic of both maps is the zero contour line, which delineates the boundary between positive and negative gradient values and is frequently regarded as the exact perimeter of a magnetic source. This is particularly advantageous in mineral exploration, as mineralization is often linked to structural features where hydrothermal solutions may have deposited ore minerals. The two maps have comparable shapes, and the distribution of their anomalies, marked by zero-contour lines, is nearly equal in place. The magnetic anomalies in both maps predominantly trend in the WNW-ESE and NE-SW orientations.

The HGM map delineates several high-gradient areas (between 7 and 43 nT/m), indicating substantial magnetic discrepancies that presumably align with lithological boundaries, faults, and potentially dykes. The prevailing orientations run northeast-southwest and northwest-southeast, indicating intricate structural influences. Areas of clustered high gradients may indicate intersections of structures or lithologies richer with magnetic properties. Regions with reduced gradients (green-blue) probably indicate homogeneous or weakly magnetic lithologies, or deeper origins.

By analyzing the structural components derived from residual, regional, FVD, TDR, and HGM maps, one may correlate structural patterns with mineralization processes and improve the interpretation of the geological framework. The rose diagrams indicate that the predominant structural trends from shallow to deep depths are predominantly NW and NE, with secondary trends originating from these two being less pronounced. The two trends and their derivatives in southern Sinai are attributable to the structural elements linked to the opening of the Gulf of Suez and the Gulf of Aqaba. Numerous discoveries related to significant mineralization, such as copper in the El Regeita area, have precipitated on shear zones and the walls of intermediate dykes due to the infiltration of hydrothermal solutions. Additionally, pegmatite dykes in certain locations are associated with high radiometric anomalies, as observed in the Khosh El Dabba area (Yousef, 2024). The extensive intermediate and pegmatite dykes in southern Sinai are predominantly associated with the northwest and northeast directions and their derivatives.

The Euler deconvolution map calculates the depths of magnetic connections throughout the survey area, employing color symbols to denote several ranges: green (shallow, <30 m), red (middle, 30-100 m), and black (deep, >100 m). The concentrated array of solutions underscores an intricate subsurface featuring many magnetic connections ranging from shallow to deep. The Source Parameter Image (SPI) map depicts shallow sources in magenta/red and deeper sources in blue, facilitating the visualization of extensive structural trends. The Euler (SI=0) and SPI maps mutually enhance each other: the Euler identifies specific contacts and depths, whilst the SPI illustrates regional depth discrepancies. The alignment between superficial Euler solutions and shallow SPI regions indicates near-surface structures, whereas deeper correlations endorse interpretations of subsurface features. Discrepancies, such as superficial Euler solutions overlapping with deeper SPI zones, may indicate local complexities, potential data noise, interference, or noise, necessitating more examination.

Gamma-Ray Spectrometric Data

The four gamma-ray spectrometric maps revealed that the high radioelement concentrations are primarily associated with alkali feldspar granites, intermediate dyke walls, and altered rock formations, indicating possible hydrothermal alteration, mineralized veins, or intrusions rich in radioactive materials. Moderate levels predominantly manifest in the central and northeastern regions, presumably associated with partially weathered or altered felsic rocks. Low values predominate in the southeastern and southern regions of the map. These diminished readings may signify structural depressions or drainage areas, where erosion or leaching has decreased the concentration of radioactive materials. A northwest-southeast oriented pattern of alternating high and low radioelement zones indicates the existence of structural lineaments or faults affecting radioelement distribution. Elongated anomalies, particularly in the central-western region, may signify dykes or vein systems enriched with uranium and thorium. Simultaneously, irregular, spot-like anomalies may signify localized mineralization pockets or alteration halos, potentially associated with intrusive bodies. Regarding the U-index, the values over 2 were contoured to identify areas of significant alteration and mineralization. According to F-parameter, the values varies from 1.2 to 1.3, indicating equilibrium distributions of these elements within prevalent rock-forming minerals. Conversely, hydrothermally altered or weathered rocks frequently display markedly increased F-values, typically ranging from 2 to 5, and occasionally reaching 10, attributable to the selective mobilization and enrichment of uranium or the depletion of thorium and potassium during alteration processes (Efimov, 1978; Wilford *et al.*, 1997; IAEA, 2003). This fluctuation underpins the application of the F-parameter in geological and mineral exploration, especially in the detection of alteration zones and uranium deposits. Figure (7d) illustrates the F-parameter map of the research area, indicating the regions of significant modification (exceeding 2.0).

Composite maps for U, Th, and K augment comprehension of elemental distribution and facilitate the identification of geochemical anomalies. The uranium map delineates regions of elevated uranium concentrations and areas exhibiting high eU/eTh and eU/K ratios, perhaps associated with uranium-rich lithologies, alteration zones, or rare earth element (REE) potential. The thorium map illustrates Th-enriched areas linked to resistate minerals such as monazite and xenotime, which are prevalent hosts for rare earth elements (REE). The potassium map (Fig. 8d) illustrates elevated potassium concentrations and potassic alteration zones, frequently associated with felsic intrusions. Collectively, these maps offer essential insights into prospective rare earth element mining areas by highlighting overlapping anomalies of uranium, thorium, and potassium.

A map was generated to integrate the gamma-ray spectrometric data, delineating the greatest values as a contour line for eU/eTh, eU/K, uranium index, and F-parameter, as previously described. A map was created from the aggregate of these contours, illustrating the zones with the highest potential for mineral development, particularly for rare earth elements (REE).

Gamma-ray spectrometry is a surface geophysical technique proficient at detecting areas of radioactive mineralization at or near the surface; nevertheless, it fails to offer insights into the depth extent or subsurface continuity of these mineralization. Consequently, to elucidate the potential extension of radioactive anomalies at depth, it is imperative to incorporate an additional geophysical method that is responsive to subsurface characteristics. Considering that radioactive mineralization may be geologically linked to metallic minerals, such as sulfides, the Self-Potential (SP) approach was chosen to augment gamma-ray spectrometry. The survey area for the SP measurements was meticulously selected to align with surface radioactive anomalies identified by gamma-ray spectroscopy. This comprehensive method improves the capacity to follow mineralized zones from surface indicators into the subsurface.

Self-Potential (SP) Data

The SP contour map enables the classification of the study area into three separate zones. Zone 1 comprises regions with SP values beneath -10.0 mV, predominantly located in the center and northwestern sections of the survey area. These zones presumably signify considerable metallic mineralization, particularly linked to the walls of the intermediate dyke. Zone 2, characterized by SP values from -10.0 to -2.0 mV, encircles the first zone. These anomalies are likely ascribed to structural characteristics such as faults, minor streams, and lithological interfaces (between intermediate dykes and altered quartz monzonite). Zone 3 corresponds to regions with SP values greater than -2.0 mV. These values indicate the existence of refractory, unmineralized rock formations.

CONCLUSION

The integration of ground magnetic, gamma-ray spectrometric, and self-potential (SP) studies in the Wadi Um Qeisum region has proven effective in delineating mineralization zones at both surface and subsurface levels. The studied area features intricate geological formations, modified granitic rocks, and intermediate dykes that significantly influence mineral occurrences. The magnetic data, analyzed through including reduction to the pole (RTP), residual and regional separation, first vertical derivative (FVD), tilt derivative (TDR), horizontal gradient magnitude (HGM), Euler deconvolution, and source parameter imaging (SPI), disclosed notable structural trends primarily oriented in NW-SE and NE-SW directions. These structures denote fault systems and lithological boundaries that govern the formation of mineralized zones.

Gamma-ray spectrometric data provide further understanding of the distribution of radioactive elements. Maps depicting equivalent uranium (eU), equivalent thorium (eTh), and potassium (K), alongside their ratios including eU/eTh, eU/K, uranium favorability index (U-Index), and the F-parameter, facilitated the identification of hydrothermal alteration zones and possible rare earth element (REE) enrichment. The radiometric anomalies exhibited spatial correlation with the intermediate dyke walls and altered quartz monzonite, underscoring their importance as exploration targets.

The SP survey provides a comprehensive perspective by mapping the subsurface continuation of surface radiometric anomalies. The SP data identified three primary zones based on potential values: significant negative anomalies indicating considerable metallic

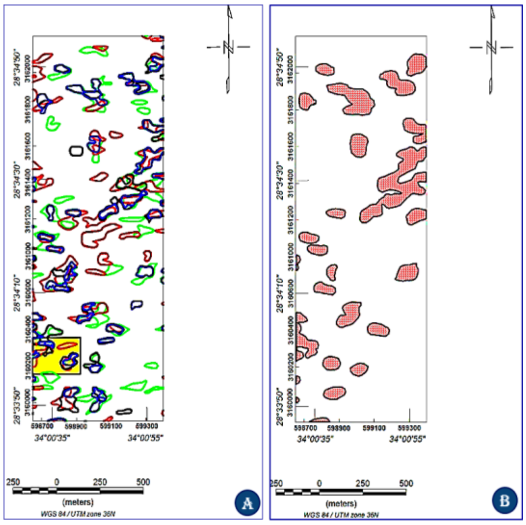

Figure (10): A, Anomaly map for eU/eTh (black), eU/K (red), eU-index (green), and F-parameter (blue), showing the selected area for the SP survey highlighted in yellow color; B, high anomalous zones, Wadi Um Qeisum, Southern Sinai, Egypt.

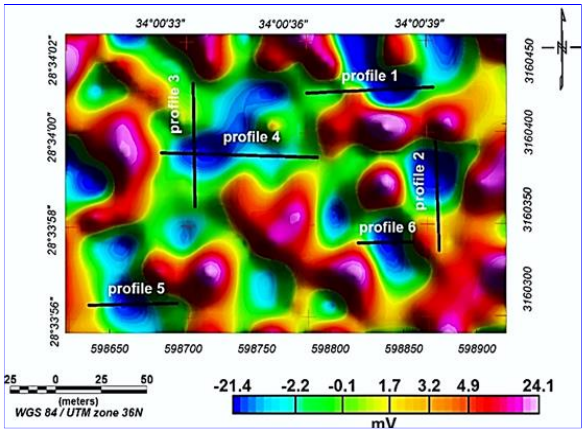

Figure (11): Spatial Potential (SP) interpolated color map with six-transect profiles , Wadi Um Qeisum, Southern Sinai, Egypt.

mineralization, intermediate anomalies linked to structural characteristics, and positive anomalies connected with unmineralized, resistive bodies. Quantitative modeling of six SP anomalies validated the existence of shallow conductive sources at depths of 9 to 14 meters characterized by moderate dip angles and limited lateral extent.

The study advocates for the execution of field geophysical investigations, including self-potential, electromagnetic, and induced polarization methods, in regions exhibiting gamma-ray spectrometric anomalies linked to significant structural trends identified through gamma-ray spectrometry and magnetic surveys. This area is particularly noteworthy due to the presence of sulfide and copper mineralization, as indicated by prior research.

ACKNOWLEDGEMENT

The authors thankfully acknowledge Dr. Ibrahim M. M. Al-Alfy and Dr. Hussein F. Abd El Salam (Nuclear Materials Authority) for their support in acquiring geophysical survey data. The authors also acknowledge the Cultural Affairs and Missions Sector, Ministry of Higher Education, Egypt, for facilitating the channel mission of Remon N. Aziz to Tohoku University as a visiting PhD research scholar.

REFERENCES

ABD EL-RAHMAN, M. A., MOHAMED, H. A., & HASSAN, A. M. 2024. Radiological Assessment of Rare Metal-Bearing Granites Using Gamma-Ray Spectrometry. Journal of Radioanalytical and Nuclear Chemistry. https://doi.org/10.1007/s10967-024-09852-5.

ABDELSALAM H. F., YOUSEF, M. H. M., SHAHEEN, M. A., BADR, H. M., EL-HAWARY, A. M., and AL-ALFY I. M. 2024. Integration of geoelectric and electromagnetic methods to delineate subsurface mineralization in bostonite rocks, South El-Atshan area, Central Eastern Desert, Egypt. Contributions to Geophysics and Geodesy. 54(2), 191-212. https://doi/10.31577/congeo.20-24.54.-2.4.

ABU EL-ELA, F., and MOHAMED, F. H. 2015. Rare earth element potential in the hydrothermal alteration zones of Wadi Um Qeisum, Sinai Peninsula, Egypt. Ore Geology Reviews, 65, 613-629.

ABUZIED, S. M., 2011. Geology and mineralization of Gebel Nakhla area, Southern Sinai, Egypt. M.Sc. Thesis, Geology Department, Suez Canal University, Ismailia, Egypt, 223 p.

AL RAWAHI, Z., AL LAWATI, H., & AL-FARSI, M. 2022. Gamma-Ray Spectrometry for Geophysical and Mineralogical Investigations. Minerals, 12(3), 294. https://doi.org/10.3390/min12030294.

ARNOUS, M. O. 2000. Integrated remote sensing and GIS investigation of mineralization in Saint Catherine area, south Sinai, Egypt. M.Sc. Thesis. Faculty of Science, Suez Canal University, Ismailia, Egypt, 125 p.

ASSRAN A. S. M., YOUSEF M. H. M., HASSAN N. F., ABD EL SALAM H. F., 2018. Self-potential, electromagnetic and gamma-ray spectrometric studies for Abu-Shihat area, North Eastern Desert, Egypt. Egypt. J. Appl. Geophys., 17(2), 1-12.

AZER, M. K., 2007. The Petrogenesis of late Precambrian felsic alkaline magmatism in south Sinai, Egypt. Acta Geologica Polonica, Vol. 56, 463-484.

AZZAZY, A.A. 2023. Mapping of hydrothermal alteration zones around wadi zubeir, northern eastern desert, Egypt using airborne gamma-ray spectrometric, aeromagnetic and remote sensing data. Journal of Egyptian Geophysical Society. 21. 21-37. 10.21608/jegs.2023.385857.

BARBOSA, V., SILVA, J.B.C., MEDEIROS, W.E., 1999. Stability analysis and improvement of structural index estimation in Euler deconvolution. Geophysicists 64, 48–60.

BENHAMOU, M., LAHRACH, A., and ABDERRAHIM, E. M. 2024. Structural and mineralogical implications of integrated ground magnetic data in the Bou Azzer inlier, Anti-Atlas, Morocco. Minerals, 14(8), 788. https://doi.org/10.3390/min14080788.

BIGALKE J., JUNGE A., ZULAUF G. 2004. Electronically conducting brittle-ductile shear zones in the crystalline basement of Rittsteig (Bohemian Massif, Germany): Evidence from self-potential and hole to surface electrical measurements. Int. J. Earth Sci., 93, 1, 44-51, doi: 10.1007/s00531-003-0364-5.

BLAKELY, R.J. 1995. Potential Theory in Gravity and Magnetic Applications. Cambridge University Press, Cambridge. http://dx.doi.org/10.1017/CBO9780511549816.

BOYLE, R. W. 1982. Geochemical prospecting for thorium and uranium deposits. Elsevier.

CHURCH B. N., 1984 Geology and self-potential survey of the Sylvester K gold-sulphide prospect (82E/2E). In: Geological fieldwork, 1983. A summary of field activities: British Colombia Ministry of Energy, Mines and resources paper 1984-1, pp. 7-14.

DARNLEY, A. G. 1973. Airborne gamma-ray techniques-present and future, In uranium exploration methods. International Atomic Energy Agency (IAEA), Proc. of a Panel, Vienna, Austria, 1972, pp. 67-108.

DARNLEY, A. G. 1973. Uranium prospecting using geochemical and radiometric techniques. Geological Survey of Canada, Economic Geology Report 31.

DREW, L. J., SCHUENEMEYER, J. H., & SUTPHIN, D. M. 2013. Uranium Deposits in Magmatic and Metamorphic Rocks, An Assessment of Favorability. USGS Scientific Investigations Report 2012-5577.

EFIMOV, M. D. 1978. Radiogeochemistry. Nedra Publishing, Moscow.

EL AREF, M. M., REFAAT, A. A., & EL-HADDAD, A. A. 1999. Hydrothermal mineralization associated with shear zones in the Saint Catherine area, South Sinai, Egypt. Geological Society of Egypt Bulletin, 72, 25-42.

EL GHAWABY, M.A., MOSTAFA, M.E., EL SHAMY, I.Z., KHAWASIK, S.M., SHENDI, E.H. AND EL MONSIF, H. (1989). Integration of remote sensing and aerogeophysics for groundwater exploration in Wadi El Arish. Proc. 2nd. Conf. Geol. Sinai Develop., Ismailia, Egypt.

EL GHRABAWY, O., ISMAIL, A., METWALY, M., MOSTAFA, A. M., 2021. Interpretation of aerospectrometric, aeromagnetic and geochemical data, Um-Alhuweitat basin area, Central Eastern Desert, Egypt. Appl Radiat Isot. 170:109477. doi: 10.1016/j.apradiso.2020.109477.

EL GHAWABY, M. A., 1984. Image linear analytical approach to copper mineral exploration in south Sinai, Egypt. International Atomic Agency, United Nations Educational, Scientific and Cultural Organization.

ELKATTAN E. M., ADULHADI H. M., RABIE S. I., HASSANEIN H. I. E., 1996. Application of ground geophysical data to uranium mineralization in the El-Missikat area, central Eastern Desert, Egypt. J. Afr. Earth Sci., 22, 1, 81-91, doi: 10.1016/0899-5362(95)00120-4.

EL QOT, G., SOLIMAN, M., AL-AFGHANI, M., & ABOUD, E. 2023. Delineation of chromite mineralization zones using ground magnetic survey in the El-Rubshi area, Central Eastern Desert, Egypt. Geoscience Letters, 10, 16. https://doi.org/10.1186/s40562-023-00298-3.

FOX R. W., 1830. On the electromagnetic properties of metalliferous veins in the mines of Cornwall. Philos. Trans. R. Soc. Lond., 120, 399{414, doi: 10.1098/rstl.1830.0027.

GEOSOFT 2014. Oasis Montaj Gridding (p. 21). Toronto: Geosoft Oasis Montaj.

GOBASHY, M.M., EL-SADEK, M.A., MEKKAWI, M.M. *ET AL*. 2024. Radiometric characteristics of some metallic ores and nonmetallic deposits: an example, Wadi Al-Allaqi, South Eastern Desert, Egypt. Sci Rep 14, 2443. https://doi.org/10.1038/s41598-024-52912-9.

GONZÁLEZ, M., PÉREZ, E., & GARCÍA, S. 2018. Applications of gamma-ray spectrometry in mining exploration. Geophysical Prospecting, 66(1), 109-119.

GRASTY, R.L., GLYNN, J.E., AND GRANT, J.A., 1985: The analysis of multichannel airborne gamma ray spectra. Geophysics, 50:2611–2620.

GRASTY, R. L., AND COX, J. R. 1997: A review of gamma-ray spectrometric data processing techniques for the determination of uranium concentration in the ground. Journal of Geochemical Exploration, 60(2), 161–176. https://doi.org/10.1016/S0375-6742(97)00033-8.

GERIESH, M., ARNOUS, M., MOHAMED, M., ABDELGAWAD, H. 2025. 'Management of Waterlogging Problem for Sustainable Land Development in Urban Areas: An Example from the North-East Cairo Region, Egypt', Catrina: The International Journal of Environmental Sciences, 35(1), pp. 29-44. doi: 10.21608/cat.2025.29-3769.1292.

HASSEN O. S., 1987: Geology and mineralization of El-Regeita area, Central south Sinai, Egypt. M.Sc thesis, Fac. Sci., Suez Canal Univ., Ismailia, Egypt.

HELMY, H. M., and KAINDL, R. 2002: Gold mineralization in the Arabian-Nubian Shield: A case study from Wadi Um Qeisum, South Sinai, Egypt. Mineralogy and Petrology, 74(1-2), 91-108.

HILMY, M.E., AND MOHSEN, L.A. 1965: Secondary copper minerals from West Central Sinai. J Geol., UAR, pp. 91-12.

HILMY, M. E. AND MOHSEN, L. A., 1966: Geology of some occurrences of copper minerals in Sinai, Ain Shams, Science Bulletin, Vol. 9, pp. 512-539.

HORO D., PAL S. K., SINGH S., BISWAS A., 2023: New insights into the gold mineralization in the Babaikundi-Birgaon Axis, North Singhbhum Mobile Belt, Eastern Indian Shield using Magnetic, Very Low-Frequency Electromagnetic (VLF-EM), and self-potential data. Minerals, 13, 10, 1289, doi: 10.3390/min13101289.

IAEA 2003: Guidelines for Radioelement Mapping Using Gamma Ray Spectrometry Data. International Atomic Energy Agency, IAEA-TECDOC-1363. Vienna, Austria.

IAEA 2010: Quantitative Analysis of Radioelement Data from Natural Sources. International Atomic Energy Agency, IAEA-TECDOC-1613. Vienna, Austria.

JOHNSON, P. R., WOLDEHAIMANOT, B., and STERN, R. J. 2011. Development of the Arabian-Nubian Shield: Perspectives on accretion and deformation in the northern East African Orogen and the assembly of Gondwana. Geological Society, London, Special Publications, 357(1), 1-20.

KEARY, P. AND BROOKS, M. 1991. An Introduction to Geophysical Exploration. 2nd Edition, Blackwell Scientific Publications, Oxford, 254 p.

LI, M., ZHOU, X., GAMMONS, C. H., KHALIL, M., SPEECE, M., 2018. Aeromagnetic and spectral expressions of rare earth element deposits in Gallinas Mountains area, Central New Mexico, USA. Interpretation (2018) 6 (4): T937-T949. https://doi.org/10.1190/INT-2017-0199.1.

MILLER, H.G., SINGH, V., 1994. Potential field tilt a new concept for location of potential field sources. J. Appl. Geophys. 32, 213-217. https://doi.org/10.1016/0926-9851 (94)90022-1.

MINTY, B. R. S., FRANKLIN, R., and MILLIGAN, P. R. 2009. Geophysical Characterisation of Australia's Regolith Using Airborne Gamma-Ray Spectrometry and Magnetic Data. In: Anand, R. R. & de Broekert, P. (Eds.), Regolith Landscape Evolution Across Australia. CRC LEME, Perth, pp. 53–75.

MOSTAFA, M.E. AND ZAKIR, F.A. 1996. New Enhancement Techniques for Azimuthal Analysis of Linearnents for Detecting Tectonic Trends in and around the Afro-Arabian Shield. International Journal of Remote Sensing, 17, 2923-2943. https://doi.org/10.1080/01431169608949119.

MOUSA, S. E. A., ELSAYED R. A. M., KHALIL A. F., ABD EL-NABI S. H.,YOUSEF M. H. M., 2014.

Delineating Cu-U mineralized zone in Wadi El-Regeita area, Southern Sinai-Egypt, using gamma-ray spectrometry and self-potential methods. EGS J. 13, 1,115-125.

NIAZY, E. A., SHALABY I. M., ABDEL RAHIM S. H., 1995. Wallrock alteration associated with the copper mineralization of Wadi El-Regeita, Southern Sinai, Egypt. Ann. Geol. Surv. Egypt, 20, 433-450.

OUADIF, L., BAHI, L., and EL AMRANI, E. M. 2022. Integration of Remote Sensing and Airborne Gamma-Ray Spectrometry for Mineral Exploration. Applied Sciences, 12(3), 957. https://doi.org/10.3-390/app12030957.

POUR, A. B., PARSA, M., ELDOSOUKY, A.M. 2023. Geospatial Analysis Applied to Mineral Expl-oration. Elsevier. 307 p. DOI: 10.1016/C2021-0-02624-9.

RASHED, M. and SHENDI, E. 2022. Construction of a 3D Conceptual Model of Subsurface Sulfide Mine-ralizations Using Integrated Geoph-ysical Survey in Saint Catherine, South Sinai, Egypt. Journal of Scientific Research and Reports 28 (1):23-34. https://doi.org/10.973-4/jsrr/2022/v2-8i130484.

REID, A.B., ALLSOP, J., GRANSER, H., MILLETT, A.T., SOMERTON, I., 1990. Magnetic interpre-tation in three dimensions using Euler decon-volution. Geophysics 55, 80–91.

RIBEIRO, A., MARTINS, L., and COSTA, D. 2020. Integration of geophysical methods for rare earth element exploration. Minerals, 10(6), 525.

SALEM, H. M. AND EL FOULY, A. A., 2000. Minerals reconnaissance at Saint Catherine area, southern central Sinai, Egypt and their enviro-nmental impacts on human health, ICEHM 2000, Cairo University, Egypt, pp. 586-598.

SALEM, A., WILLIAMS, S., FAIRHEAD, J. D., RAVAT, D. AND SMITH, R., 2007. Tilt-depth method: A simple depth estimation method using first order magnetic derivatives, The Leading Edge, 26, pp. 1502-1505.

SAUNDERS, D.F., POTTS, M.J., 1978. Manual for application of NURE 1974–1977 aerial gamma-ray spectrometric data: U.S. Department of Energy, Grand Junction office, Report GJBX–13(87), 183 p.

SANTOS, F., ROCHA, M., and OLIVEIRA, A. 2016. Self-potential methods in mineral exploration: App-lications and challenges. Geophysical Surveys, 42(1), 58-72.

SHALABY, M. H., EL MAHALLAWI, M. M., and ASRAN, A. M. 2005. Geology and mineralization of the Precambrian rocks in the Saint Catherine area, Sinai Peninsula, Egypt. Journal of African Ea-rth Sciences, 41(2), 175-190.

SHARMA, P.V. 1997. Environmental and Engineering Geophysics. Cambridge University Press, Cam-bridge, 1-475. http://dx.doi.org/10.1017/CBO978-1139171168.002.

SHENDI, E. H 1992. Gamma-ray spectrometry of po-rphyry calcalkaline rocks of Wadi Sidud area, south Sinai. 3rd Conference on the Geology of Sinai for development, Ismailia, Egypt, Proceedings, pp. 49-54.

STERN, R. J. 1994. Arc assembly and continental coll-ision in the Neoproterozoic East African Oro-gen: Implications for the consolidation of Gond-wana-land. Annual Review of Earth and Planetary Sciences, 22(1), 319-351.

SULTAN A. S., MANSOUR S. A., SANTOS F. M., HELALY A. S., 2009. Geophysical exploration for gold and associated minerals, case study: Wadi El Beida area, South Eastern Desert, Egypt. J. Geop-hys. Eng., 6, 4, 345-356, doi: 10.1088/17422132-/6/4/002.

THURSTON, J.B. AND SMITH, R.S. 1997. Automatic Conversion of Magnetic Data to Depth, Dip, and Susceptibility Contrast Using the SPITM Method. Geophysics, 62, 807-813.

WILFORD, J. R., BIERWIRTH, P. N., and CRAIG, M. A. 1997. Application of airborne gamma-ray spectrometry in environmental mapping and expl-oration. AGSO Journal of Australian Geology and Geophysics, 17(2), 201-216.

WILFORD, J. R. 2012. A Weathering intensity index for the Australian continent using airborne gamma-ray spectrometry and digital Terrain analysis. Geoscience Australia, Record 2012/29. Canberra: Geoscience Australia.

YOUSEF, M. H. M. 2024. The structural elements controlling the subsurface mineralization as deduced from the integration of magnetic and self-potential methods, Wadi Khosh El-Daba area, southern Sinai, Egypt. Contributions to Geophysics and Geodesy Vol. 54/3, 2024 (279-300). doi: 10.31577/congeo.2024.54.3.4.

تطبيق الطرق الجيوفيزيائية الأرضية لتحديد مناطق التمعدن: دراسة حالة في وادي أم قيسوم، منطقة سانت كاترين، جنوب سيناء، مصر

ريمون ناجح عزيز[1]، محمد حسن يوسف[1]، عادل فهمى خليل [1]، صلاح محمد حنفى[1]، موتويوكى ساتو[3]، العربى هندى شندى[2]
[1] قطاع الاستكشاف، هيئه المواد النوويه، القاهره، مصر
[2] قسم الجيولوجيا، كلية العلـــــوم، جامعه قناه السويس، الاسماعيليه مصر
[3]جامعه طوهوكو، سنداى، اليابان

الملخــص العــربي

وادي أم قيسوم، الواقع في منطقة سانت كاترين بجنوب سيناء، مصر، يقع ضمن الدرع العربي النوبي ويحتوي على مجموعة متنوعة من الموارد الطبيعية، بما في ذلك النحاس، وعناصر الأرضية النادر (REEs) ، وأيضا المواد المشعة. يجمع هذا البحث بين المسوحات المغناطيسية الأرضية، والمسوحات الإشعاعية، وتقنيات الجهد الذاتي (SP) لتحديد مناطق التمعدنات وتحليل تأثيراتها البنائيه. تم تحليل البيانات المغناطيسية باستخدام منهجيات تشمل الاختزال إلى القطب (RTP)، والفصل بين الشاذات القريبة والبعيدة عن السطح، المركبه العموديه الاولى(FVD) ، المشتقه الكليه(TDR) ، والمشتقه الافقيه (HGM) ، ومعامل الشكل (SI = 0) ، الإستنباط التصويري لعناصر المصدر. وطريقه الحث الكهربي قد حسنت التعرف على الفوالق، والجدد، والاتصالات التي تحكم التمعدن، والتي تتميز بالاتجاهات البنائيه السائدة NW-SEو .NE-SW حدد قياس الطيف بالأشعة السينية عدم انتظام في توزيعات eU و eTh و .K المؤشرات المستمدة (eU/eTh، eU/K، U-Index، F-parameter) والخرائط الثلاثية الأبعاد حددت مناطق التغيير الهيدروحراري وإمكانية إثراء العناصر الأرضية النادرة. تتوافق الشاذات الإشعاعية مع جدران الفوالق المتوسطة، والكوارتز مونزونيت المتحول، والتقاطعات البنائيه. بياناتSP ، التي تم الحصول عليها من 16 خطا، حددت ثلاث مناطق: شاذات سلبية ملحوظة (‎-10.0 >) مللي فولت مرتبطة بتكثيف معدني كبير؛ شاذات متوسطة (‎-10.0 إلى ‎-2.0 مللي فولت) مرتبطة بالخصائص البنائيه؛ وشاذات إيجابية (‎-2.0 <) مللي فولت تشير إلى مناطق مقاومة غير معدنية. أظهر النمذجة الكمية مصادر ضحلة (بعمق-9-14 متر) تتميز بانحدارات منخفضة ومدى جانبي محدود. تكامل هذه التقنيات يحدد بدقة المواقع تحت السطحية ويسهل استكشاف أماكن التمعدنات مستقبليا.